Simulation and Design of PID Position Control for a Three-Gear Torque Transmission System Using Root Locus

Rehan Pinanda Prasetia[1], Ulinnuha Latifa[2] , Marvel Aji Setiawan[3] , Muhammad Rasya[4]
[1,2,3,4] Electrical Engineering, Universitas Singaperbangsa Karawang
E-mail: 2210631160064@student.unsika.ac.id[1], ulinuha.latifa@ft.unsika.ac.id[2],[3]2210631160049@student.unsika.ac.id,
[3]2210631160056@student.unsika.ac.id

***Abstract*—This paper presents the design and simulation of a PID position control system for a three-gear torque transmission mechanism using the root locus method. Unlike many previous studies that focus on simple electromechanical plants, this work applies classical PID control to a multi-gear mechanical transmission system with load disturbance, where gear interactions influence the transient response. The system model was derived using first-principles modeling and represented by a second-order transfer function with an integrator. The uncompensated system exhibits poor transient performance, with 45.52% overshoot and a steady-state error of 0.5, failing to meet the design specifications of maximum 8% overshoot, zero steady-state error, and a settling time three times faster than the original system. A PID controller was designed using the root locus technique by placing the dominant poles at a location corresponding to a damping ratio of 0.626, resulting in controller parameters Kp = 1.989, Ki = 0.913, and Kd = 0.325. Simulation results show that the controller eliminates overshoot and achieves zero steady-state error under a 0.5 Nm load disturbance, although the settling time of 4.286 s remains longer than the desired 1.366 s. A comparison of PI, PD, and PID controllers reveals trade-offs between response speed, damping, and steady-state accuracy in multi-gear transmission systems.**

Keywords—PID control, root locus, gear transmission system, position control,, trade-off analysis.

I. INTRODUCTION

Precise position control is a fundamental requirement in many mechatronic and industrial systems that demand accurate angular motion and torque regulation [1]. Gear transmission mechanisms are widely implemented to meet these requirements due to their ability to adjust torque and speed efficiently. However, multi-stage gear systems, such as three-gear transmission mechanisms, introduce more complex dynamic interactions compared to single-stage systems. The coupling between gears, reflected inertia, and damping effects significantly influence the overall system dynamics, often resulting in degraded transient performance and sensitivity to disturbances [2].

The Proportional–Integral–Derivative (PID) controller remains one of the most widely used control strategies due to its simple structure and practical effectiveness [3]. Various studies have shown that properly tuned PID controllers can improve system performance in terms of overshoot reduction and steady-state accuracy [4]. Among available tuning methods, the Root Locus technique provides a systematic graphical approach that relates pole locations to time-domain specifications, making it a popular choice for controller design in classical control systems [1].

Despite extensive research on PID control and root locus methods, most existing studies focus on relatively simple systems such as single-actuator or low-order mechanical models. The application of these classical design techniques to multi-gear transmission systems has not been sufficiently explored. In such systems, the interaction between multiple gears introduces higher-order dynamics and additional constraints, which may limit the effectiveness of conventional controller design approaches [5].

In addition, a fundamental challenge in PID-based control is the trade-off between transient performance and steady-state accuracy. While derivative action can improve damping and speed of response, integral action is required to eliminate steady-state error caused by disturbances. However, the inclusion of integral action may introduce slow dynamics that degrade the overall system response, particularly in complex mechanical systems.

Therefore, this study aims to design and analyze a PID position control system for a three-gear torque transmission mechanism using the Root Locus method. The objective is to evaluate the ability of classical PID control to satisfy transient response specifications, including overshoot, settling time, and steady-state error, in the presence of load disturbances.

The main contributions of this paper are as follows:

1. Development of a dynamic model of a three-gear torque transmission system based on first-principles modeling.
2. Systematic design of a PID controller using the Root Locus method for a multi-gear system.
3. Comprehensive analysis of the trade-offs between PI, PD, and PID controllers in terms of speed, damping, and steady-state accuracy.
4. Identification of the limitations of root locus–based PID design in achieving fast settling time when integral action is required.

II. MATERIALS AND METHODS

This study employs a simulation-based approach to design and evaluate a position control system for a three-gear torque transmission mechanism. The overall methodology consists of system modeling, controller design using the Root Locus method, and performance evaluation through time-domain simulation.

A. System Description

The plant under study is a three-gear torque transmission system as shown in Fig. 1, where the first gear is driven by an actuator torque τ_a and the third gear delivers torque to a load with disturbance torque (T_L). This configuration consists of three spur gears in series that transmit rotational motion and torque from the input to the output shaft. Gear transmission systems are widely used in mechanical drive trains, including automotive gearboxes and industrial automation, due to their high torque-transmission capability and predictable kinematic relationships [6].

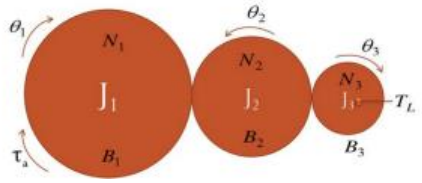


Fig. 1. Three-gear torque transmission system

In control design, gear trains are commonly modeled as interconnected rotational inertial elements whose dynamic behavior depends on the gear ratios and the inertial and damping properties of each gear. The interaction between gears introduces constraints in angular displacement and torque transfer that must be captured in the system model for accurate controller design and stability analysis [6]. The effective inertia seen at the input shaft and output shaft is a function of the gear ratios and the physical inertia and damping coefficients of all gears in the transmission.

The parameters used in this study, as summarized in Table 1, are chosen based on typical values reported in control and dynamic modeling studies and are representative of small-scale electromechanical transmission systems. Such parameter ranges have been shown to yield realistic dynamic responses in simulation studies of gear transmission systems, making them appropriate for control analysis[6]. These assumptions enable a tractable model suitable for controller design while capturing essential dynamic characteristics of the plant.

TABLE I. PLANT PARAMETERS

Parameter	Value
Teeth of Gear 1 (N_1)	36
Teeth of Gear 2 (N_2)	24
Teeth of Gear 3 (N_3)	12
Inertia of Gear 1 (J_1)	$5 \times 10^{-3} kg \cdot m^2$
Inertia of Gear 2 (J_2)	$4 \times 10^{-3} kg \cdot m^2$
Inertia of Gear 3 (J_3)	$1 \times 10^{-3} kg \cdot m^2$
Damping of Gear 1 (B_1)	$0.01\ N \cdot m \cdot \frac{s}{rad}$
Damping of Gear 2 (B_2)	$0.007\ N \cdot m \cdot \frac{s}{rad}$
Damping of Gear 3 (B_3)	$0.003\ N \cdot m \cdot \frac{s}{rad}$
Input Torque (τa)	$1\ Nm$
Disturbance of Load Torque (T_L)	$0.5\ Nm$

Real-world implementations of multi-gear torque transmission systems can be found in robotic actuators, automotive powertrains, and precision positioning equipment in manufacturing systems. In these applications, gear trains adjust torque and speed between a motor and mechanical load, and accurate control is required to achieve precise motion and robust performance under varying loads and disturbances [6].

This study considers two analysis scenarios to ensure consistency between controller design and performance evaluation. First, the controller is designed based on a nominal plant model where the load torque disturbance is neglected (TL = 0). This assumption is necessary to apply classical root locus design techniques. Second, the performance of the designed controller is evaluated under a disturbance condition by introducing a load torque of 0.5 Nm in the simulation. This separation allows a clear distinction between nominal design validation and disturbance rejection capability.

B. Mathematical Modeling

The mathematical model is derived by applying Newton's second law for rotational motion to each gear [7]. The torques acting on the gears include the input torque, the reaction torques between meshing gears (τ_{12} between gear 1 and 2, and τ_{23} between gear 2 and 3), and the damping torques. The equations of motion for each gear, where $\theta_i(t)$ is the angular position, are:

For Gear 1:

$$J_1 \frac{d^2\theta_1(t)}{dt^2} = \tau_a - \tau_{12} - B_1 \frac{d\theta_1(t)}{dt} \quad (1)$$

For Gear 2:

$$J_2 \frac{d^2\theta_2(t)}{dt^2} = \tau_{12} - \tau_{23} - B_2 \frac{d\theta_2(t)}{dt} \quad (2)$$

For Gear 3:

$$J_3 \frac{d^2\theta_3(t)}{dt^2} = \tau_{23} - T_L - B_3 \frac{d\theta_3(t)}{dt} \quad (3)$$

The kinematic relationships between the gears, considering their teeth ratios and opposite directions of rotation, are derived from the gear geometry [8]:

$$\frac{\theta_1}{\theta_2} = -\frac{N_1}{N_2} \Rightarrow \theta_1 = -\frac{N_1}{N_2}\theta_2 \quad (4)$$

$$\frac{\theta_3}{\theta_2} = -\frac{N_3}{N_2} \Rightarrow \theta_2 = -\frac{N_2}{N_3}\theta_3 \quad (5)$$

By combining (4) and (5), the relationship between the input gear (Gear 1) and the output gear (Gear 3) can be established. The intermediate torques τ_{12} and τ_{23} can be eliminated by substituting equations (1), (2), and (3) and using the gear ratios [9]. The process involves reflecting the inertias and dampings of gears 2 and 3 to the input shaft of gear 1, or vice versa, to obtain an equivalent system [7]. After algebraic manipulation and simplification, the entire three-gear system can be represented as a single equivalent rotational body at the output shaft (Gear 3). The resulting equation of motion, with the T_L considered as a disturbance, is:

$$\tau_a - TL = J_{eq}\frac{d^2\theta_3(t)}{dt^2}(t) + B_{eq}\frac{d\theta_3(t)}{dt} \quad (6)$$

Where J_{eq} and B_{eq} are the equivalent moment of inertia and equivalent viscous damping coefficient reflected to the output shaft (Gear 3). These equivalent parameters are functions of the individual gear parameters and their respective gear ratios. By substituting the numerical values from Table 2.1 into the expressions for J_{eq} and B_{eq}, the equation of motion becomes:

$$\tau_a - TL = 0.062\frac{d^2\theta_3(t)}{dt^2}(t) + 0.121\frac{d\theta_3(t)}{dt} \quad (7)$$

Equation (7) is the final mathematical model of the three-gear system in the time domain. This model describes the dynamic relationship between the input torque τ_a, the disturbance load torque T_L, and the output angular position θ_3. The subsequent section will transform this model into the frequency domain to obtain the transfer function for control system analysis and design.

C. Transfer Function Derivation

For the purpose of control system analysis and design, it is convenient to represent the system dynamics in the frequency domain using a transfer function. The transfer function is defined as the ratio of the Laplace transform of the output variable to the Laplace transform of the input variable, assuming zero initial conditions[10]. In this study, the output variable is the angular position of the third gear ($\theta_3(t)$), and the primary input is the actuator torque ($\tau_a(t)$), with the load torque ($T_L(t)$) considered as an external disturbance.

Starting from the time-domain mathematical model derived in the previous section (Equation 7):

$$0.062\frac{d^2\theta_3(t)}{dt^2}(t) + 0.121\frac{d\theta_3(t)}{dt} = \tau_a - T_L \quad (8)$$

Taking the Laplace transform of both sides of Equation (8) and assuming zero initial conditions ($\theta_3(0) = 0, \dot{\theta}_3(0) = 0$), we obtain the algebraic equation in the complex frequency domain s [9]:

$$0.062s^2\theta_3(s) + 0.121s\theta_3(s) = \tau_a(s) - T_L(s) \quad (9)$$

Equation (9) can be rearranged to express the output $\theta_3(s)$ as a function of the two inputs:

$$(0.062s^2 + 0.121s)\theta_3(s) = \tau_a(s) - T_L(s) \quad (10)$$

$$\theta_3(s) = \frac{1}{0.062s^2 + 0.121s}\tau_a(s) - \frac{1}{0.062s^2 + 0.121s}T_L(s) \quad (11)$$

Equation (11) shows that the system response is a superposition of the responses to the actuator torque and the load torque disturbance. For controller design purposes, the load torque disturbance T_L is initially neglected (TL = 0) to obtain the nominal transfer function of the plant. This approach is commonly used in classical control design, where disturbances are treated separately during performance evaluation [7]. This yields the transfer function from the input torque $\tau_a(s)$ to the output angular position $\theta_3(s)$:

$$P(s) = \frac{\theta_3(s)}{\tau_a(s)} = \frac{1}{0.062s^2 + 0.121s} \quad (12)$$

The transfer function in Equation (12) is in a raw form based on the physical parameters. For easier analysis and implementation in standard control system tools, it is often normalized. Factoring out the coefficient of the highest power of s in the denominator, the transfer function can be rewritten as:

$$P(s) = \frac{\frac{1}{0.062}}{s^2 + \frac{0.121s}{0.062}} \quad (13)$$

Performing the numerical division yields the simplified form of the open-loop transfer function:

$$P(s) = \frac{16.13}{s^2 + 1.952s} \quad (14)$$

This transfer function $P(s)$ represents the dynamics of the three-gear torque transmission system from the actuator input to the angular position output. It is a type-1 system due to the presence of an integrator ($\frac{1}{s}$ term), indicating that the system will have zero steady-state error for a step input in position but a finite error for a ramp input [8]. The denominator is second-order, but the absence of a constant term confirms the presence of a pole at the origin. This transfer function forms the basis for the subsequent analysis of system characteristics (stability, transient response, steady-state error) and the design of the PID controller using root locus techniques.

D. Block Diagram Representation

A block diagram is a visual representation of a system that illustrates the flow of signals and the functional relationships between different components [10]. This section presents the block diagram representation of the three-gear torque transmission system derived from the mathematical model obtained in Sections B and C.

1) Block Diagram from Mathematical Equations

From the Laplace domain equation (Equation 7), which expresses the relationship between input torque, load disturbance, and output position, a block diagram can be constructed that explicitly shows the system's internal structure. This representation includes summing junctions, integrator blocks $\left(\frac{1}{s}\right)$, and feedback paths representing the damping effect, providing insight into how the output angular position $\theta_3(s)$ is generated from the input signals [9].

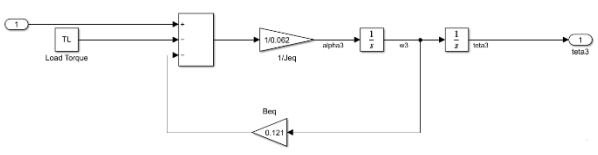


Fig. 2. Block diagram constructed from Equation (7)

Fig. 2 shows the open-loop block diagram constructed from the mathematical equations of the three-gear system, illustrating how the input torque propagates through each

gear considering their inertias, damping coefficients, and gear ratios.

For control purposes, the system can be configured in a closed-loop configuration with feedback. Fig. 3 shows the closed-loop block diagram derived from the mathematical equations, where the output angular position θ_3 is fed back and compared with the reference input. This representation includes the complete gear dynamics with feedback path [7].

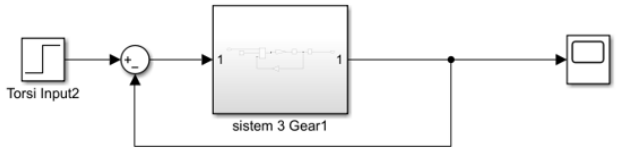


Fig. 3. Closed-loop block diagram from mathematical equations

2) Block Diagram from Transfer Function

A more compact representation can be obtained using the transfer function approach. From Equation (11), which shows the superposition of responses to actuator torque and load torque disturbance, an open-loop block diagram can be constructed. This diagram, shown in Fig. 4, illustrates how the load torque $T_L(s)$ acts as a disturbance that subtracts from the actuator input $\tau_a(s)$ before entering the plant dynamics [8].

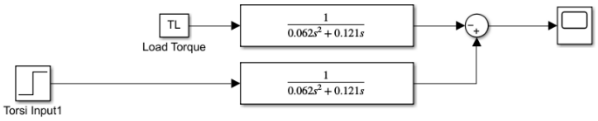


Fig. 4. Block diagram constructed from Equation (11)

For control system analysis and design, the system is typically configured in a closed loop with unity feedback. Fig. 5 shows the closed-loop block diagram without any controller, where the output position $\theta_3(s)$ is fed back and compared with a reference input $\theta_{ref}(s)$ to generate an error signal [11]. This configuration forms the basis for the controller design that will be discussed in subsequent sections.

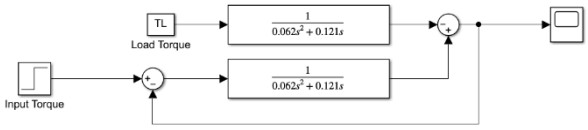


Fig. 5. Closed-loop block diagram from transfer function

These block diagrams provide the foundation for understanding the system dynamics and implementing the PID controller design using root locus techniques.

E. Transient Response Analysis

The transient response characteristics of a system describe its behavior during the transition from an initial state to a final steady-state condition. These characteristics are crucial for evaluating system performance and determining the need for controller design. This section analyzes the transient response of the three-gear torque transmission system based on the closed-loop transfer function derived in Section C.

1) Closed-Loop Transfer Function

From Section C, the open-loop transfer function of the system was derived at Equation (14). With unity feedback, the closed-loop transfer function becomes:

$$\frac{\theta_3(s)}{\theta_{ref}(s)} = \frac{P(s)}{1+P(s)} = \frac{16.13}{s^2 + 1.952s + 16.13} \tag{15}$$

This is a second-order system that can be written in the standard form:

$$\frac{\theta_3(s)}{\theta_{ref}(s)} = \frac{{\omega_n}^2}{s^2 + 2\xi\omega_n s + {\omega_n}^2} \tag{16}$$

2) Natural Frequency and Damping Ratio

Comparing Equations (15) and (16), the natural frequency ω_n and damping ratio ζ are obtained:

$$\omega_n^2 = 16.13 \Rightarrow \omega_n = \sqrt{16.13} = 4.02\frac{rad}{s} \tag{17}$$

$$2\zeta\omega_n = 1.952 \Rightarrow \zeta = \frac{1.952}{2 \times 4.02} = 0.243 \tag{18}$$

The damping ratio $\zeta = 0.243$ indicates that the system is underdamped, meaning it will exhibit oscillatory behavior before reaching steady state[11]. This relatively low damping ratio is typical in gear transmission systems where mechanical components have minimal inherent energy dissipation[12].

The damped natural frequency ω_d is:

$$\omega_d = \omega_n\sqrt{1-\zeta^2} = 4.02\sqrt{1-(0.243)^3} = 3.90\frac{rad}{s} \tag{19}$$

3) Transient Response Parameters

For an underdamped second-order system, key transient response parameters can be calculated using standard formulas [13]:

Percent Overshoot (%OS): The maximum overshoot relative to the steady-state value:

$$\%OS = e^{-\left(\frac{\zeta\pi}{\sqrt{1-\zeta^2}}\right)} \times 100\% = e^{-\left(\frac{0.243\pi}{\sqrt{1-0.243^2}}\right)} \times 100\% = 45.52\% \tag{20}$$

This relatively high overshoot indicates that the system will experience significant oscillation before settling, which may be undesirable for precise position control applications. Studies on gear system dynamics have shown that such overshoot levels can lead to increased wear and reduced positioning accuracy in multi-stage gear trains[7].

Peak Time (T_p): The time required to reach the first peak of the overshoot:

$$T_P = \frac{\pi}{\omega_d} = \frac{\pi}{3.90} = 0.806\ second \tag{21}$$

Settling Time (T_s): The time required for the response to remain within ±2% of the final value:

$$T_s = \frac{4}{\zeta\omega_n} = \frac{\pi}{0.243 \times 4.02} = 4.098\ second \tag{22}$$

This relatively long settling time suggests that the system responds slowly to input changes [12]. In gear transmission applications, settling time is a critical performance metric affecting overall system productivity [14].

Rise Time (T_r): The time required for the response to rise from 10% to 90% of the final value. For an underdamped second-order system, an approximate formula is:

$$T_r \approx \frac{1.8}{\omega_n} = \frac{1.8}{4.02} = 0.448\ second \qquad (23)$$

4) Steady-State Error with Load Disturbance

From Equation (11) in Section 2.3, the output $\theta_3(s)$ is affected by both the input torque $\tau_a(s)$ and the load torque disturbance $T_L(s)$. For a step input of $\tau_a(s) = 1/s$ and a step disturbance of $T_L(s) = 0.5/s$, the steady-state output can be found using the Final Value Theorem:

$$\theta_3(\infty) = \lim_{s\to 0} s\left[\frac{16.13}{s^2+1.952s}\cdot\frac{1}{s} - \frac{16.13}{s^2+1.952s}\cdot\frac{0.5}{s}\right] = 1 - 0.5 = 0.5 \qquad (24)$$

Thus, the load torque disturbance of 0.5 Nm introduces a steady-state error of 0.5 in the output position, even though the system would have zero error for a step input without disturbance [13]. This highlights the need for integral control action to reject steady-state disturbances.

5) Simulation Validation

To validate the analytical calculations, the dynamic behavior of the closed-loop system was first evaluated under nominal conditions without external disturbances. In this case, the load torque was neglected ($T_L = 0$), allowing the simulation to reflect the inherent dynamics of the gear transmission system and enabling direct comparison with the analytical transient response derived in the previous section. The system was simulated in MATLAB/Simulink using a step input of 1 Nm applied to the actuator torque. Fig. 6 shows the step response of the uncompensated closed-loop system without load disturbance.



Fig. 6. Step response of the uncompensated system without load torque disturbance

To evaluate the robustness of the system under realistic operating conditions, a load torque disturbance was then introduced at the output shaft. In this case, a step disturbance of $T_L = 0.5$ Nm was applied simultaneously with the reference input. This disturbance represents the external mechanical load acting on the output gear and allows the effect of disturbance on system performance to be examined. Fig. 7 shows the step response of the uncompensated system when the load torque disturbance is applied.

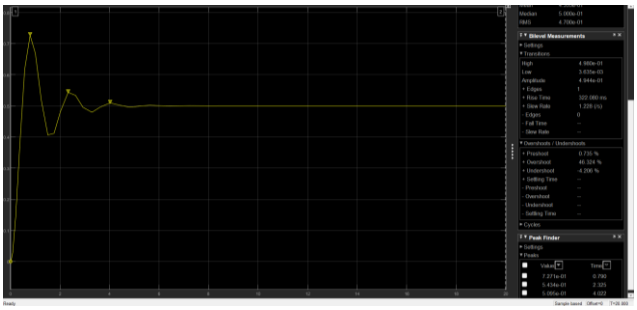


Fig. 7. Step response of the uncompensated system with load torque disturbance

TABLE II. TRANSIENT RESPONSE CHARACTERISTICS

Parameter	Analytical Calculation	Simulink Simulation (TL = 0)	Simulink Simulation (TL = 0.5)
%OS	45.52	46.32	46.32
Ts	4.098 s	3.52 s	3.80 s
Tp	0.806 s	0.803 s	0.790 s
Tr	0.448 s	0.307 s	0.322 s
$e(\infty)$	0.5	0	0.5

Table 2 compares the transient response parameters obtained from analytical calculations and Simulink simulations under two conditions: without load disturbance ($T_L = 0$)and with a load torque disturbance of $T_L = 0.5$Nm. The simulation results without disturbance show good agreement with the analytical predictions. For example, the percent overshoot obtained analytically is 45.52%, while the simulation produces 46.32%, and the peak time is 0.806 s analytically compared to 0.803 s in simulation. These close values indicate that the derived mathematical model accurately represents the system dynamics.

When the load disturbance is introduced, the overshoot remains nearly unchanged at approximately 46.32%, while the settling time increases slightly from 3.52 s to 3.80 s due to the additional torque load acting on the output gear. In addition, the steady-state error becomes 0.5, indicating that the uncompensated system cannot reject constant load disturbances [14]. These results highlight the need for a controller with integral action to eliminate steady-state error and improve the overall system performance.

6) Desired Transient Response Spesifications

The current transient response characteristics do not meet acceptable performance criteria for precise position control applications. Therefore, a controller must be designed to improve the system response. Table 3 summarizes the desired transient response specifications that will guide the controller design.

TABLE III. DESIRED TRANSIENT RESPONSE SPECIFICATIONS

Parameter	Target Value	Justification
Maximum Percent Overshoot (%OS)	8%	To minimize oscillation and ensure smooth position control

Settling Time (Ts)	1.366 s	Three times faster than original (4.09/3) for improved responsiveness
Steady-State Error (e(∞))	0	To eliminate the effect of load torque disturbance

These specifications require a significant reduction in overshoot (from 45% to 8%) and a threefold improvement in settling time, while maintaining zero steady-state error. Achieving these goals will require careful design of a controller using techniques such as root locus or frequency response methods.

F. PID Controller Design Using Root Locus

The root locus method is a graphical technique proposed by Evans in 1948 that utilizes the open-loop transfer function to plot the movement trajectory of the system's characteristic roots as parameters vary[2]. This method is an important tool in classical control theory and is particularly effective for system analysis and controller design, as the position, shape, and direction of the root locus in the s-plane intuitively reflect the influence of parameter variations on system behavior [2]. This section presents the design of a PID controller for the three-gear torque transmission system using the root locus approach, based on the desired specifications established in Section E: maximum overshoot of 8% and settling time three times faster than the original system (1.366 seconds).

1) Initial Root Locus Analysis

Before designing the controller, it is essential to examine the root locus of the uncompensated system [7]. The open-loop transfer function is given by Equation (14):

$$P(s) = \frac{16.13}{s^2 + 1.952s}$$

Fig. 8 shows the root locus of the uncompensated open-loop system. The system has two poles: one at $s = 0$ and one at $s = -1.952$. The root locus starts from these poles and moves along the real axis as the gain increases. The pole at the origin indicates that the system is type-1, which will result in zero steady-state error for step inputs but may cause stability issues if not properly damped[8].

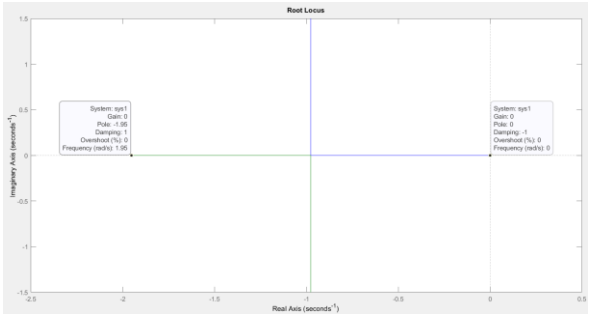


Fig. 8. Root locus of the uncompensated open-loop system

The closed-loop root locus of the uncompensated system with unity feedback is shown in Fig. 8. Here, the two poles become complex conjugates as the gain increases, indicating an underdamped response [7]. The damping ratio corresponding to the operating point can be determined from this locus.

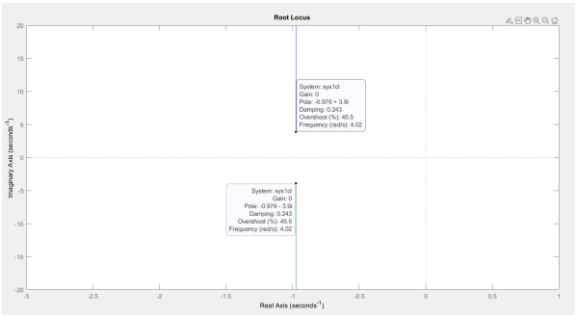


Fig. 9. Root locus of the uncompensated closed-loop system

From Fig. 9, it can be observed that the dominant poles for the uncompensated system have a damping ratio of approximately $\zeta = 0.243$, which corresponds to an overshoot of 45.5%. This confirms the analysis in Section 2.5 and highlights the need for a controller to improve the transient response[15].

2) Desired Pole Location

The desired percent overshoot of 8% corresponds to a damping ratio ζ calculated using the formula for underdamped second-order systems [16] :

$$\zeta = \frac{-\ln(\frac{\%OS}{100})}{\sqrt{\pi^2 + \left(\ln(\frac{\%OS}{100})\right)^2}} = \frac{-\ln(0.08)}{\sqrt{\pi^2 + (\ln(0.08))^2}} = 0.626 \quad (25)$$

From Section E, the original settling time was $T_s = 4.09$ seconds. The target settling time is three times faster

$$Ts_{new} = \frac{4.098}{3} = 1.366\ s \quad (26)$$

For a second-order system, the settling time is related to the real part of the dominant poles by $T_s = 4/\sigma$, where $\sigma = \zeta\omega_n$ [16]. Therefore, the required real part is:

$$\sigma = \frac{4}{Ts_{new}} = \frac{4}{1.366} = 2.928 \quad (27)$$

With $\zeta = 0.626$ and $\sigma = 2.928$, the natural frequency ω_n is:

$$\omega_n = \frac{\sigma}{\zeta} = \frac{2.928}{0.626} = 4.677\ rad/s \quad (28)$$

The imaginary part of the dominant poles is:

$$\omega_d = \omega_n\sqrt{1 - \zeta^2} = 4.677\sqrt{1 - 0.626^2} = 3.63\ rad/s \quad (29)$$

Thus, the desired dominant closed-loop poles are located at:

$$s_{1,2} = -\sigma \pm j\omega_d = -2.928 \pm j3.63 \quad (30)$$

3) PD Control Design

A PD controller adds a zero to the open-loop transfer function, allowing the root locus to pass through the desired pole location. The PD controller has the form:

$$G_{PD}(s) = s + z_c \tag{31}$$

The open-loop transfer function of the system with PD controller is:

$$G_{PD}(s)P(s) = \frac{16.13(s + z_c)}{s^2 + 1.952s} \tag{32}$$

The angle condition must be satisfied for the desired pole $s_1 = -2.928 + j3.63$. The angles from the poles of $P(s)$ at $s = 0$ and $s = -1.952$ to s_1 are calculated as follows:

For the pole at $s = 0$, the angle θ_1 is:

$$\theta_1 = \tan^{-1}\left(\frac{3.63}{2.928}\right) = 51.4° \tag{33}$$

For the pole at $s = -1.952$, the distance along the real axis is $2.928 - 1.952 = 0.976$, so:

$$\theta_2 = \tan^{-1}\left(\frac{3.63}{0.976}\right) = 75.1° \tag{34}$$

The sum of angles from the plant poles is:

$$\theta_P = \theta_1 + \theta_2 = 51.4° + 75.1° = 126.5° \tag{35}$$

For the desired pole to lie on the root locus, the angle contributed by the PD controller zero must satisfy[16]:

$$\theta_{zc} - 126.5° = 180° \Longrightarrow \theta_{zc} = 180 + 126.5 = 306.5° \; or \; equivalently \; 53.5° \tag{36}$$

Thus, the angle from the controller zero to s_1 should be 53.5°. If the zero is located at z_c on the real axis, then:

$$\tan(53.5°) = \frac{3.63}{z_c - 2.928} \tag{37}$$

Solving for z_c:

$$z_c - 2.928 = \frac{3.63}{\tan(53.5°)} = \frac{3.63}{1.35} = 2.69 \tag{38}$$

$$z_c = 2.928 + 2.69 = 5.62 \tag{39}$$

Therefore, the PD controller zero is placed at $s = -5.62$, giving:

$$G_{PD}(s) = s + 5.62 \tag{40}$$

Fig. 10 shows the root locus after adding the PD controller. The locus is now modified to pass through the desired pole location $s = -2.928 \pm j3.63$ at a specific gain. The zero at $s = -5.62$ attracts the root locus, allowing the desired damping ratio to be achieved.

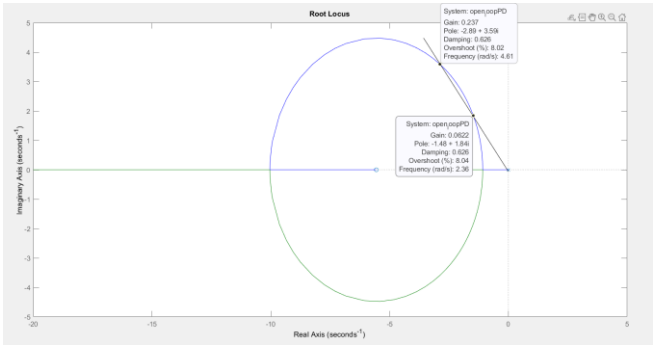


Fig. 10. Root locus after adding PD controller

4) PI Control Design

The PD controller improves transient response but does not eliminate steady-state error [17]. A PI controller adds an integrator and a zero to eliminate steady-state error while maintaining the desired transient response. The PI controller has the form:

$$G_{PI}(s) = \frac{s + z_i}{s} \tag{41}$$

The zero of the PI controller is typically placed close to the origin so that the integral action can effectively eliminate steady-state error while minimizing its influence on the dominant transient dynamics [16]. Placing the zero near the origin ensures that the controller mainly improves low-frequency performance without significantly altering the dominant pole locations determined during the root locus design stage. Following common practice in classical controller design, the PI zero in this study is selected at $z_i = 0.5$, which provides sufficient integral action while maintaining acceptable transient characteristics [17]. Thus:

$$G_{PI}(s) = \frac{s + 0.5}{s} \tag{42}$$

5) Complete PID Controller

The complete PID controller is the product of the PD and PI controllers with a gain K:

$$G_{PID}(s) = K \cdot G_{PD}(s) \cdot G_{PI}(s) = K \cdot \frac{(s + 5.62)(s + 0.5)}{s} \tag{43}$$

Expanding the numerator:

$$G_{PID}(s) = K \cdot \frac{s^2 + 6.12s + 2.81}{s} \tag{44}$$

The gain K is determined from the magnitude condition on the root locus at the desired pole location $s_1 = -2.928 + j3.63$. The magnitude of the loop gain must equal 1:

$$\left| K \cdot \frac{(s_1 + 5.62)(s_1 + 0.5)}{s_1(s_1 + 1.952)} \right| = 1 \tag{45}$$

Calculating each term:

- $|s_1| = \sqrt{2.928^2 + 3.63^2} = 4.67$

- $|s_1 + 1.952| = |-0.976 + j3.63| = \sqrt{0.976^2 + 3.63^2} = 3.76$
- $|s_1 + 0.5| = |-2.428 + j3.63| = \sqrt{2.428^2 + 3.63^2} = 4.37$
- $|s_1 + 5.62| = |2.692 + j3.63| = \sqrt{2.692^2 + 3.63^2} = 4.52$

The product of magnitudes from the plant poles in the denominator is:

$$|s_1| \cdot |s_1 + 5.62| = 4.67 \times 3.76 = 17.56$$

The product of magnitudes from the controller zeros in the numerator is:

$$|s_1 + 0.5| \cdot |s_1 + 5.62| = 4.37 \times 4.52 = 19.75$$

Thus:

$$K\frac{19.75}{17.56} = 1 \Longrightarrow K = \frac{19.75}{17.56} = 0.325 \quad (46)$$

The complete PID controller transfer function is therefore:

$$G_{PID}(s) = \frac{0.325(s^2 + 6.12s + 2.81)}{s} = \frac{0.325s^2 + 1.989s + 0.913}{s} \quad (47)$$

Fig. 11 shows the root locus of the system with the complete PID controller. The dominant poles are placed at the desired location according to the root locus design procedure, which theoretically corresponds to the targeted transient response specifications. However, the complete closed-loop system contains additional poles and zeros introduced by the PID controller, which may influence the actual transient response obtained in simulation. The addition of the PI controller zero at $s = -0.5$ and the pole at the origin ensures zero steady-state error while maintaining the desired damping ratio [16].

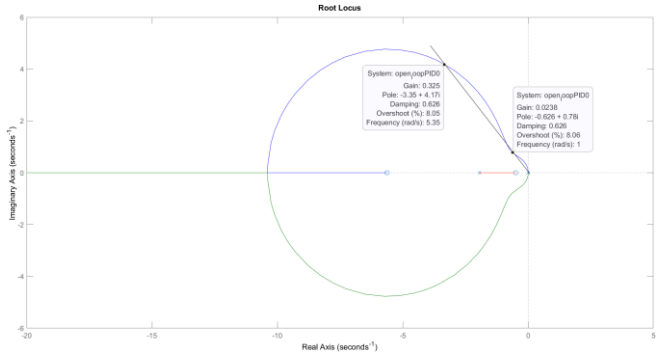


Fig. 11. Root locus of the PID-compensated system

6) PID Parameters

Comparing with the standard PID form $G_c(s) = K_p + \frac{K_i}{s} + K_d s = \frac{K_d s^2 + K_p s + K_i}{s}$, the PID parameters are obtained [16] :

$$K_p = 1.989, \quad K_i = 0.913, \quad K_d = 0.325 \quad (48)$$

Fig. 12 shows the complete block diagram of the system with the PID controller, including the load torque disturbance T_L [8].

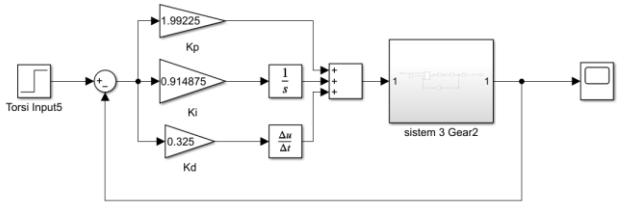


Fig. 12. Block diagram of the three-gear system with PID controller

7) Discussion of the Design

The root locus design method presented here follows a systematic two-step approach: first designing a PD controller to place the dominant poles at the desired location, then adding a PI controller to eliminate steady-state error. This approach is particularly effective for electrical servomechanisms and gear transmission systems where both transient response and steady-state accuracy are critical [15].

The controller obtained is essentially a two-degree-of-freedom PID controller, where the PD portion handles the transient response and the PI portion ensures zero steady-state error. The zero placed at $s = -0.5$ in the PI controller is sufficiently close to the origin to not significantly alter the transient response while providing the necessary integral action[16].

The gain $K = 0.325$ ensures that the desired poles are exactly on the root locus. However, as noted in Section 2.5, the actual settling time may differ from the theoretical value due to the presence of additional poles and zeros from the controller, as well as the effect of the load torque disturbance[8]. The performance of this designed controller will be evaluated through simulation in Section 3.

III. Results And Discussion

. This chapter presents the simulation results of the three-gear torque transmission system controlled by PI, PD, and PID controllers designed using the root locus method in Chapter 2. The transient responses of each controller are analyzed and compared with the uncompensated system and the desired specifications established in Section E. The simulations were conducted using MATLAB/Simulink to validate the theoretical design and assess the contribution of each control action (proportional, integral, derivative) to the system's performance under load torque disturbance.

A. Simulation Setup

To evaluate the performance of the designed controllers, a simulation model was developed in MATLAB/Simulink. This section describes the simulation parameters, controller configurations, and input signals used in the study.

1) Simulink Model Configuration

The block diagram shown in Fig. 11 was implemented in Simulink to simulate the closed-loop system with each controller configuration. The plant transfer function represents the three-gear torque transmission system as derived in Equation (14):

$$P(s) = \frac{16.13}{s^2 + 1.952s}$$

The system parameters used in the simulation are consistent with those listed in Table 1, including the load torque disturbance of $T_L = 0.5$ Nm applied at the output shaft.

Three controller configurations were implemented for comparison:

1. **PI Controller:** Based on the design in Equation (42), the PI controller transfer function is:

$$G_{PI}(s) = \frac{s + 0.5}{s}$$

with the gain $K = 0.325$ applied as in the full PID controller to maintain consistency.

2. **PD Controller:** Based on the design in Equation (40), the PD controller transfer function is:

$$G_{PD}(s) = s + 5.62$$

with the same gain $K = 0.325$.

3. **PID Controller:** The complete PID controller designed in Equation (47) has the transfer function:

$$G_{PID}(s) = \frac{0.325s^2 + 1.989s + 0.913}{s}$$

which corresponds to the PID gains:

$$K_p = 1.989, \qquad K_i = 0.913, \qquad K_d = 0.325$$

2) Input Signals and Simulation Parameters

The simulation was configured with the following parameters to evaluate the system's response under realistic operating conditions:

- **Reference input:** A step input of magnitude 1 radian ($\theta_{ref}(s) = 1/s$) was applied as the desired position command. This represents a typical scenario where the gear system must rotate to a target angular position.
- **Load torque disturbance:** A step disturbance of $T_L = 0.5$ Nm was applied at $t = 0$ to simulate the effect of external load on the output gear. This disturbance represents the torque required to drive the load connected to Gear 3.
- **Simulation time:** The simulation was run for 30 seconds, which is sufficient to observe the complete transient response and steady-state behavior for all controller configurations.
- **Solver settings:** The variable-step ode45 (Dormand-Prince) solver was used with a relative tolerance of 1×10^{-3} to ensure accurate numerical integration while maintaining computational efficiency.

3) Performance Metrics

To quantitatively evaluate and compare the controller performance, the following transient response parameters were extracted from the simulation results using MATLAB's stepinfo function:

- **Rise Time (T_r):** The time required for the response to rise from 10% to 90% of the final steady-state value.
- **Settling Time (T_s):** The time required for the response to remain within ±2% of the final steady-state value.
- **Percent Overshoot ($\%OS$):** The maximum peak value relative to the steady-state value, expressed as a percentage.
- **Peak Time (T_p):** The time at which the first peak of the overshoot occurs.
- **Steady-State Error ($e(\infty)$):** The difference between the desired reference and the actual output after the transient has settled.

These metrics provide a comprehensive basis for comparing the performance of PI, PD, and PID controllers against the uncompensated system and the design specifications.

B. Simulation Results of PID-Controlled System

This section presents the step response of the three-gear torque transmission system with the designed PID controller. The simulation was conducted according to the setup described in Section A, with a step reference input of 1 radian and a load torque disturbance of 0.5 Nm applied at t = 0.

1) Step Response with Load Torque Disturbance

Fig. 13 shows the step response of the PID-controlled system under the load torque disturbance of 0.5 Nm. The output angular position $\theta_3(t)$ is plotted against time, demonstrating the system's ability to track the reference input despite the presence of the disturbance.

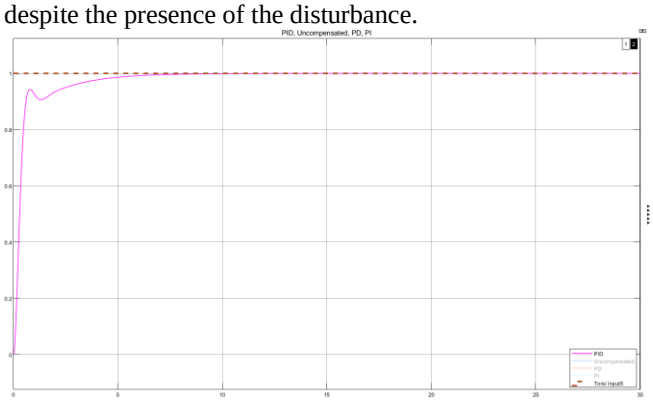


Fig. 13. Step response of the PID-controlled system with load torque disturbance (0.5 Nm)

Fig. 13 presents the step response of the three-gear torque transmission system when controlled using the designed PID controller under a load torque disturbance of 0.5 Nm. The signal shape shows a smooth and monotonic rise toward the reference value without oscillatory behavior. Unlike the underdamped response observed in the uncompensated system, the output trajectory increases gradually and approaches the steady-state value without crossing the reference level. This indicates that the controller successfully modifies the system dynamics to produce a well-damped response.

From the waveform characteristics, the response initially rises relatively quickly and then gradually approaches the

final value with a slow convergence phase. This signal shape is typical of systems with significant integral action, where the integral component continues to accumulate the error until the steady-state condition is achieved. As a result, the output eventually reaches the reference value with zero steady-state error, demonstrating the controller's capability to compensate for the constant load torque disturbance applied to the system.

However, the overall waveform also reveals that the settling phase occurs slowly, as the response takes several seconds before entering the steady-state region. The absence of oscillations indicates that the system is strongly damped, but the relatively long settling period suggests that the dominant closed-loop poles are positioned closer to the imaginary axis than expected. Consequently, while the PID controller effectively improves stability and disturbance rejection, the signal shape indicates a trade-off where improved damping leads to a slower transient response.

2) Transient Response Parameters

The transient response parameters extracted from the simulation are summarized in Table 4. These values were obtained using MATLAB's stepinfo function and verified through visual inspection of the response curve.

TABLE IV. TRANSIENT RESPONSE PARAMETERS OF THE PID-CONTROLLED SYSTEM

Parameter	Symbol	Value
Rise Time (10% to 90%)	Tr	0.5026 *s*
Settling Time (2% criterion)	Ts	4.17 *s*
Percent Overshoot	%OS	0%
Steady-State Error	$e(\infty)$	0

The results in Table 4 demonstrate that the PID controller achieves zero overshoot, which is well below the target maximum of 8%. The steady-state error is eliminated entirely, achieving the target of zero error. However, the settling time of 4.17 s is notably longer than the desired target of 1.366 s.

The rise time of 0.5026 s indicates that the initial response is reasonably fast, but the prolonged settling time suggests that the system continues to creep toward the final value for an extended period. This behaviour is characteristic of systems where the integral action introduces slow dynamics that dominate the later portion of the transient response.

3) Comparison with Uncompensated System

To better understand the improvement achieved by the PID controller, Fig. 14 compares the step response of the uncompensated system (without controller) and the PID-compensated system under the same load torque disturbance of 0.5 Nm.

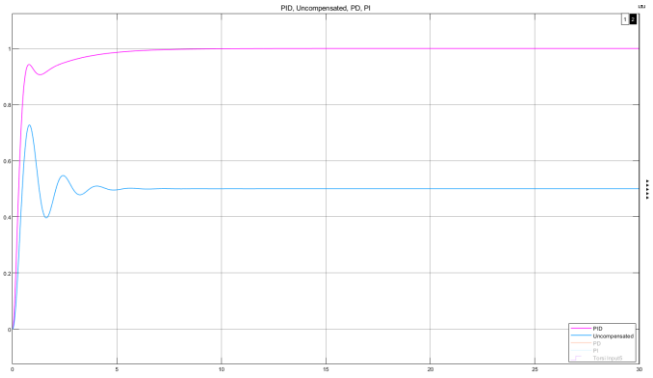


Fig. 14. Comparison of step responses: uncompensated vs. PID-controlled system

The blue signal, which represents the uncompensated system, exhibits a large overshoot followed by noticeable oscillations around the reference value. The response rises rapidly, exceeds the desired position, and then oscillates several times before gradually approaching the steady-state value. This waveform indicates an underdamped system with insufficient damping, where the dominant poles produce oscillatory dynamics and poor transient performance.

In contrast, the purple signal, representing the PID-controlled system, shows a significantly different waveform. The response increases smoothly toward the reference value without exceeding it, resulting in a monotonic signal shape with no oscillations. This behavior indicates that the PID controller effectively increases the damping of the closed-loop system, suppressing the oscillatory characteristics observed in the uncompensated response. Consequently, the system reaches the desired position in a more stable and controlled manner.

However, the comparison between the two signals also reveals a trade-off in dynamic performance. While the purple PID-controlled signal successfully eliminates overshoot and oscillations, it approaches the steady-state value more gradually than the blue uncompensated signal. This slower convergence is visible in the longer tail of the response curve before reaching steady state. Such behavior suggests that the controller prioritizes stability and disturbance rejection over response speed, which is commonly observed in systems where integral action plays a dominant role in eliminating steady-state error.

Table 5 provides a quantitative comparison between the uncompensated and PID-controlled systems using the new parameter set.

TABLE V. COMPARISON OF UNCOMPENSATED AND PID-CONTROLLED SYSTEMS

Parameter	**Uncompensated**	**PID**	**Improvement**
%OS	45.52	0	Reduced to zero
Ts	3.5247 *s*	4.2861 *s*	Increased by 0.7614 s
Tr	0.3137 *s*	0.5026 *s*	Increased by 0.1889 s
$e(\infty)$	0.5	0	Eleminated

The comparison reveals that the PID controller achieves substantial improvement in overshoot reduction and steady-

state error elimination. The overshoot is completely eliminated, far exceeding the 8% specification. The steady-state error is eliminated, which is essential for precise position control applications where load disturbances are present.

However, the settling time shows an increase of 0.7614 seconds compared to the uncompensated system, indicating that the controller did not improve the speed of response. This finding is significant because one of the design objectives was to achieve a settling time three times faster than the original (1.366 s). The actual settling time of 4.2861 s is approximately 3.05 times slower than the target and also slower than the uncompensated system.

The rise time also shows an increase from 0.3137 s to 0.5026 s, suggesting that the PID controller slows the initial response while providing superior damping. This trade-off between speed and damping is well-documented in control systems literature and reflects the inherent limitations of fixed-gain controllers when multiple performance objectives must be satisfied.

4) Summary of PID Controller Performance

The simulation results demonstrate that the PID controller designed using the root locus method successfully achieves two of the three design objectives:

1. The percent overshoot is reduced to 0%, meeting the ≤8% specification.
2. The steady-state error is eliminated, achieving the zero-error target.

However, the settling time of 4.2861 s falls significantly short of the 1.366 s target, indicating that the desired speed of response was not achieved. One major reason for this discrepancy is the presence of the integral zero placed at $s = -0.5$in the PI component of the PID controller. Zeros located close to the origin tend to introduce slow dynamic modes that influence the later portion of the transient response [17]. As a result, although the root locus design places the dominant poles at locations corresponding to faster theoretical dynamics, the overall closed-loop response may still converge slowly toward the steady state.

Another contributing factor is the limitation of the dominant pole approximation used in classical root locus–based design. The analytical estimation of settling time assumes that the system behavior can be represented by a second-order model dominated by a pair of complex poles [16]. In practical systems, especially mechanical transmission systems with multiple inertias and damping elements, additional dynamics may appear and influence the transient response [6]. These additional dynamics can produce slower modes that extend the settling phase of the response compared with the theoretical prediction.

Consequently, while the PID controller effectively improves damping and eliminates steady-state error, the achieved settling time remains longer than the target specification. Similar limitations have been observed in studies of multi-stage gear transmission systems where complex mechanical interactions influence the dynamic response of the system [14]. These results indicate that additional controller refinement, such as adjusting the location of the integral zero or applying alternative tuning strategies, may be required to achieve faster transient performance.

C. Comparison of PI, PD, and PID Controllers

To understand the contribution of each control action to the system's performance, this section compares the step responses of the system with PI, PD, and PID controllers. The simulations were conducted under the same conditions described in Section A: step reference input of 1 radian and load torque disturbance of 0.5 Nm applied at t = 0. The controller parameters are derived from the root locus design in Chapter 2, with the PI controller using the zero at s = -0.5, the PD controller using the zero at s = -5.62, and the PID controller combining both with gain K = 0.325.

1) Analysis of PI Controller Response

Fig. 15 shows the step response of the system with PI controller compared to the uncompensated system.

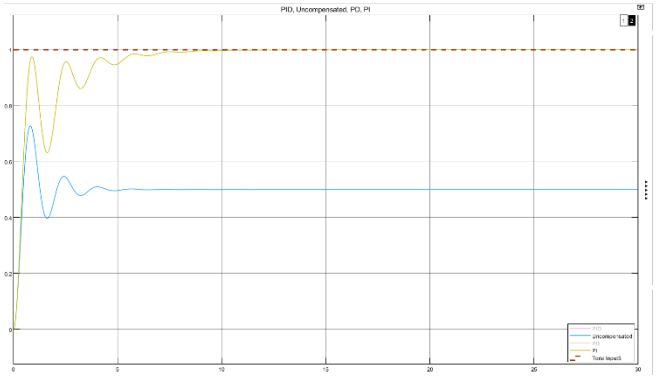


Fig. 15. Step response of PI Controller

Fig. 15 shows the step response of the system using the PI controller compared with the uncompensated system under the same load torque disturbance. The yellow signal, which represents the PI-controlled response, initially rises rapidly and exhibits a noticeable overshoot followed by damped oscillations before gradually approaching the reference value. The waveform indicates that the PI controller improves the steady-state tracking capability of the system, as the response eventually converges to the reference level, demonstrating the effect of the integral action in reducing steady-state error. However, the signal still shows several oscillations during the transient phase, suggesting that the system remains underdamped and that the PI controller alone does not provide sufficient damping to fully suppress oscillatory behavior, unlike the smoother response achieved with the PID controller.

2) Analysis of PD Controller Response

Fig. 16 shows the step response of the system with PD controller compared to the uncompensated system.

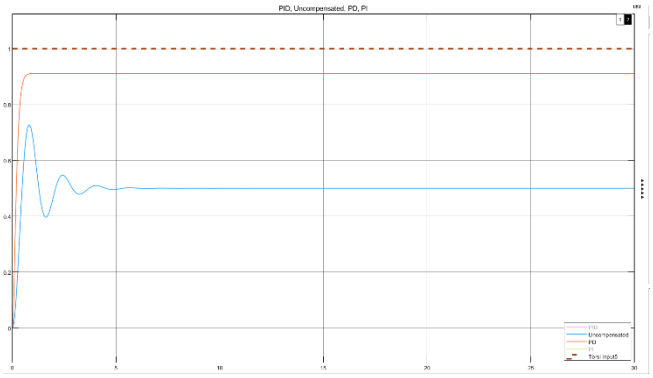


Fig. 16. Step response of PD Controller

Fig. 16 shows the step response of the system using the PD controller compared with the uncompensated system under the same load torque disturbance. The orange signal, representing the PD-controlled response, rises toward the reference value with reduced oscillations compared to the uncompensated system, indicating that the derivative action improves the damping characteristics of the system. Although the response still exhibits a small overshoot, the amplitude of oscillation is significantly lower than that of the uncompensated response, and the waveform settles more smoothly toward the steady-state region. However, unlike the PI and PID controllers, the PD-controlled signal does not completely eliminate the steady-state error because the controller lacks an integral component to compensate for constant disturbances such as the applied load torque.

3) Overall Comparison of Response

Fig. 17 presents all four responses (uncompensated, PI, PD, and PID) on a single plot for direct comparison.

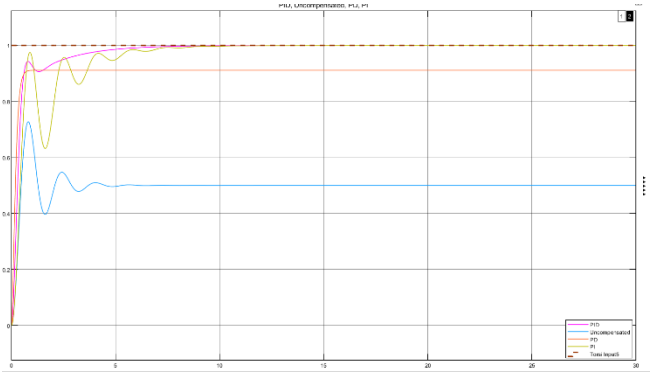


Fig. 17. PD Controller Overall comparison of uncompensated, PI, PD, and PID responses

Fig. 17 presents the comparison of the step responses of the PI, PD, and PID controlled systems under the same load torque disturbance. The yellow signal (PI controller) shows a noticeable overshoot followed by several damped oscillations before gradually reaching the steady-state value, indicating that although the integral action improves steady-state accuracy, the system remains underdamped during the transient phase. The orange signal (PD controller) exhibits reduced oscillations and faster initial response compared with the PI controller, demonstrating that the derivative action improves system damping and transient behavior; however, the response does not fully reach the reference value due to the absence of integral action to eliminate steady-state error. In contrast, the purple signal (PID controller) shows the smoothest waveform, rising gradually toward the reference value without overshoot and settling steadily at the desired position, indicating that the combined proportional, integral, and derivative actions provide improved damping and steady-state accuracy compared with the PI and PD controllers individually.

4) Quantitative Analysis of Transient Parameters

Table 6 summarizes the transient response parameters extracted from the simulation data for each controller configuration.

TABLE VI. COMPARISON OF UNCOMPENSATED AND PID-CONTROLLED SYSTEMS

Controller	**Rise Time (Tr)**	**Settling Time (Ts)**	**Overshoot (%OS)**	**Steady-State Error ($e(\infty)$)**
Uncompensated	0.3117	3.5251	45.52	0.5
PI	0.5387	6.6181	0	0
PD	0.3289	0.5617	≈ 0	0.0888
PID	0.4948	4.2861	0	0

The quantitative data confirm the visual observations from the step responses. Several key findings emerge:

- **Overshoot performance:** Both PI and PID controllers achieve zero overshoot, meeting the design specification of ≤8%. The PD controller also achieves virtually zero overshoot, indicating excellent damping from derivative action. The uncompensated system's 45.52% overshoot confirms the need for control.
- **Steady-state accuracy:** PI and PID controllers achieve zero steady-state error, satisfying the design requirement. The PD controller retains an error of 0.0888, which may be acceptable in applications where speed is prioritized over absolute accuracy. The uncompensated system's error of 0.5 demonstrates the significant impact of load disturbance.
- **Speed of response:** The PD controller is fastest by a substantial margin, with settling time of 0.5617 s—approximately 6.3 times faster than the uncompensated system. The PID controller's settling time of 4.2861 s is 22% slower than uncompensated, while the PI controller is 88% slower. This reveals that integral action, while necessary for steady-state accuracy, significantly degrades response speed.
- **Rise time:** The uncompensated achieves the fastest rise time (0.3117 s), followed by PD (0.3289 s), PID (0.4948 s), and PI (0.5387 s). The rise time ranking differs from settling time ranking because rise time measures only the initial response, while settling time includes the entire transient.

5) Comparison with Previous Studies

The results obtained in this study can be compared with previous works that applied PID control to mechanical and electromechanical systems. The designed PID controller achieves zero overshoot (0%) and zero steady-state error, but produces a settling time of 4.2861 s, which is longer than the desired target of 1.366 s. This indicates that although the controller successfully improves damping and disturbance

rejection, the transient response speed remains limited. Similar behavior is commonly observed in classical PID control when integral action is introduced to eliminate steady-state disturbances.

Comparable findings have been reported in PID-based position control systems. Juarsa et al. reported that PID controllers are effective in reducing overshoot and achieving accurate steady-state tracking in DC motor positioning systems, although the resulting transient performance strongly depends on system parameters and tuning methods [4]. In addition, studies on multi-stage gear transmission systems have shown that complex mechanical interactions between gears can introduce additional dynamic modes that influence the transient response and extend the settling phase of the system [14]. These observations are consistent with the results obtained in this study, where the PID controller improves damping and steady-state accuracy but does not fully achieve the desired settling time specification.

6) Discussion of Trade-Offs

The quantitative analysis reveals several fundamental trade-offs inherent in linear time-invariant feedback control. These trade-offs explain the performance differences observed among the four controller configurations and provide important insights for practical control system design. The comparison reveals fundamental trade-offs in control system design:

- **The Speed-Accuracy Trade-Off:** Controllers that eliminate steady-state error tend to exhibit slower transient responses. The PD controller achieves the fastest settling time (0.5617 s) but retains a small steady-state error (0.0888). In contrast, both PI and PID controllers eliminate steady-state error through integral action but produce significantly longer settling times (6.6181 s and 4.2861 s, respectively). This behavior occurs because integral action improves low-frequency gain for disturbance rejection but introduces slower dynamics in the transient response.
- **The Damping-Speed Trade-Off:** Increasing damping to reduce overshoot generally reduces response speed. The uncompensated system exhibits a fast rise time (0.3117 s) but suffers from excessive overshoot (45.52%). Derivative action improves damping significantly, allowing the PD controller to achieve negligible overshoot while maintaining a relatively fast response. However, when integral action is added, the transient response becomes slower despite the improved steady-state accuracy.
- **The Integral-Derivative Trade-Off:** Integral and derivative actions provide complementary advantages. Integral control eliminates steady-state error but introduces slower dynamics, while derivative control improves damping and response speed but cannot fully reject constant disturbances. The PID controller combines these actions, achieving zero steady-state error and zero overshoot, but with an intermediate settling time.
- **The Zero Location Trade-Off:** The location of controller zeros also influences transient behavior. The PI zero placed near the origin contributes to eliminating steady-state error but introduces a slow dynamic mode that prolongs settling. In contrast, the PD zero located farther from the origin mainly affects the early transient response, improving rise time and damping.

. Overall, these trade-offs explain why the PID controller successfully eliminates overshoot and steady-state error but does not achieve the targeted settling time of 1.366 s. Achieving faster settling performance while maintaining accuracy may require further controller refinement, such as adjusting zero placement, applying lead–lag compensation, or adopting more advanced control strategies.

D. Potential Improvement Strategies

Although the PID controller designed using the root locus method successfully eliminates steady-state error and overshoot, the results indicate that the controller cannot simultaneously satisfy all transient response specifications. In particular, the obtained settling time of 4.2861 s remains significantly larger than the target value of 1.366 s, indicating that the current controller configuration is not optimal for achieving fast transient performance in the three-gear torque transmission system.

One possible improvement is retuning the PID parameters, particularly by adjusting the location of the integral zero. Moving the zero farther from the origin can reduce the slow dynamic mode introduced by integral action and potentially improve the settling performance of the system [17]. Another classical approach is the use of lead or lead–lag compensation, which can shift the dominant poles further to the left in the complex plane and improve transient response speed [16].

In addition to classical techniques, optimization-based tuning methods have been widely used to determine PID parameters that simultaneously satisfy multiple performance criteria such as overshoot, settling time, and steady-state accuracy [14]. Such methods allow automatic exploration of parameter combinations that may achieve better overall performance compared to manual tuning approaches.

More advanced control structures may also be considered in future work. For example, two-degree-of-freedom PID controllers allow independent tuning of reference tracking and disturbance rejection characteristics, which can improve settling performance without sacrificing steady-state accuracy [15].

Therefore, while the classical root locus–based PID controller provides a useful baseline design, further refinement of the controller structure and parameter selection may be required to achieve faster transient response while maintaining system stability and accuracy.

IV. CONCLUSION

This study presented the design and simulation of a PID position control system for a three-gear torque transmission mechanism using the root locus method. The dynamic model of the system was derived from first-principles modeling and represented by a second-order transfer function with an integrator. Simulation results showed that the uncompensated system exhibited poor transient performance, with 45.52% overshoot and a steady-state error of 0.5 under load disturbance.

The designed PID controller with parameters $K_p = 1.989$, $K_i = 0.913$, and $K_d = 0.325$ successfully improved the system performance by eliminating overshoot and

achieving zero steady-state error under a load torque disturbance of 0.5 Nm. However, the obtained settling time of 4.2861 s was longer than the desired target of 1.366 s, indicating that the designed controller satisfies two of the three design objectives. The results also revealed important trade-offs between speed, damping, and steady-state accuracy, where the inclusion of integral action improves disturbance rejection but introduces slower transient dynamics.

Future work may focus on improving the transient response by optimizing the placement of controller zeros or applying advanced control strategies such as lead–lag compensation, optimization-based PID tuning, or two-degree-of-freedom PID structures to achieve a better balance between response speed and accuracy.

REFERENCES

[1] Y. K. Wiguna, P. W. Rusimamto, B. Suprianto, and M. S. Zuhrie, "Desain Sistem Pengendali Posisi Sumbu Azimuth Pada Turret Gun Dengan PI Controller Metode Root-Locus," *JURNAL TEKNIK ELEKTRO*, vol. 10, no. 3, pp. 817–825, Sep. 2021, doi: https://doi.org/10.26740/jte.v10n3.p817-825.

[2] E. P. Fadillah, Endryansyah, P. W. Rusimamto, and M. S. Zuhrie, "Desain Sistem Pengaturan Keseimbangan Posisi Bola pada Sistem Ball and Beam Menggunakan Metode Kendali Root Locus Berbasis MATLAB," *Jurnal Teknik Elektro*, vol. 11, no. 1, pp. 136–145, Jun. 2022, doi: doi.org/10.26740/jte.v11n1.p136-145.

[3] R. Solekha and U. Latifa, "Sistem Kendali Proportional Integral Derivative (PID) Menggunakan Mikrokontroler Arduino Pada Thinkercad," *Electron : Jurnal Ilmiah Teknik Elektro*, vol. 5, no. 1, pp. 89–96, May 2024, doi: https://doi.org/10.33019/electron.v5i1.108.

[4] D. Juarsa, M. Fadli, and E. R. Susanto, "Rancang Bangun Modul Kontrol Berbasis PID untuk Pengaturan Kecepatan dan Posisi Motor DC Menggunakan STM32 dan Rotary Encoder," *INSOLOGI: Jurnal Sains dan Teknologi*, vol. 4, no. 4, pp. 845–859, Aug. 2025, doi: 10.55123/insologi.v4i4.6081.

[5] Q. A. Fiddina, W. H. Pramujati, and A. S. C. Buana, "Tuning PID Control using GEO Algorithm for Dual Axis Sun Tracker System," *Jurnal Kridatama Sains dan Teknologi*, vol. 7, pp. 18–35, Jan. 2025, doi: https://doi.org/10.53863/kst.v7i01.1485.

[6] Y. Zeng, J. Zhu, Y. Han, D. Qiu, W. Huang, and M. Xu, "Dynamic Modeling and Numerical Analysis of Gear Transmission System with Localized Defects," *Machines*, vol. 13, no. 4, Apr. 2025, doi: 10.3390/machines13040272.

[7] W. Lu, G. Liang, Z. Du, W. Huang, and X. Zhao, "Dynamic coupling effects of geometric eccentricity on multi-stage gear transmission via stiffness modulation and error excitation," *Sci. Rep.*, Dec. 2025, doi: 10.1038/s41598-025-33768-z.

[8] R. Tuirán, H. Maury, H. Águila, J. Oñate, and H. Álvarez, "Hybrid dynamic model of spur gears under combined misalignments," *Advances in Mechanical Engineering*, vol. 17, no. 9, Sep. 2025, doi: 10.1177/16878132251380302.

[9] J. Ding and G. Jin, "Modeling and dynamic analysis of split torsion transmission system considering backlash and center distance errors," *Sci. Rep.*, vol. 15, no. 1, p. 1229, 2025, doi: 10.1038/s41598-024-81753-9.

[10] G. Mo, C. Liu, G. Liu, and F. Liu, "Improved Nonlinear Dynamic Model of Helical Gears Considering Frictional Excitation and Fractal Effects in Backlash," *Machines*, vol. 13, no. 4, p. 262, Mar. 2025, doi: 10.3390/machines13040262.

[11] D. Sheng, J. Yang, and C. Su, "Dynamic Analysis and Fatigue Life Evaluation of Single Herringbone Planetary Gear System with Crack Fault," *Journal of Mechanical Engineering Science and Technology (JMEST)*, vol. 9, no. 1, p. 26, Mar. 2025, doi: 10.17977/um016v9i12025p026.

[12] B. B. Pejovic, B. Ćirković, and D. Ljamić, "Determination of dynamic effects in machine tools during the transient period by applying the reduction system method," 2010. [Online]. Available: https://api.semanticscholar.org/CorpusID:111937192

[13] T. Żabiński and L. Trybus, "Tuning P-PI and PI-PI controllers for electrical servos," *Bulletin of The Polish Academy of Sciences-technical Sciences*, vol. 58, pp. 51–58, 2010, [Online]. Available: https://api.semanticscholar.org/CorpusID:55811017

[14] Y. Yi, X. Tan, L. Xuan, and C. Liu, "Dynamic Interaction Behavior of an Electric Motor Drive Multistage Gear Set," *IEEE Access*, vol. PP, p. 1, Apr. 2020, doi: 10.1109/ACCESS.2020.2985665.

[15] P. Tzouganakis, V. Gakos, C. Papalexis, C. Kalligeros, A. Tsolakis, and V. Spitas, "Non-dimensional control for robust vibration attenuation during acceleration in coaxial magnetic gears," *Meccanica*, vol. 61, no. 1, p. 29, 2026, doi: 10.1007/s11012-026-02091-w.

[16] M. Bahtiar *et al.*, "Penentuan Konstanta PID Sistem Kendali Satelit Sumbu X, Y, dan Z Menggunakan Metode Root Locus," *Jurnal Ilmiah Teknik Elektro*, vol. 20, no. 1, pp. 68–80, 2022, doi: 10.25105/jetri.v20il.13473.

[17] J. Cvejn, "The magnitude optimum design of the PI controller for plants with complex roots and dead time," *Archives of Control Sciences*, pp. 5–35, Apr. 2022, doi: 10.24425/acs.2022.140862.